Electronic Supplementary Information

Highly Stretchable Hydrogels for UV Curing Based High-Resolution Multimaterial 3D Printing

*Biao Zhang, [a†] Shiya Li, [a†] Hardik Hingorani,[a†] Ahmad Serjouei, [a] Liraz Larush, [b] Amol A. Pawar, [b] Wei Huang Goh, [a] Amir Hosein Sakhaei, [a] Michinao Hashimoto, [a] Kavin Kowsari, [a] Shlomo Magdassi *[bc] and Qi Ge *[ad]*

a. Digital Manufacturing and Design Centre, Singapore University of Technology and Design, 487372, Singapore.

b. Casali Centre for Applied Chemistry, Institute of Chemistry, The Centre for Nanoscience and Nanotechnology, The Hebrew University of Jerusalem, Jerusalem 9190401, Israel.

c. Singapore-HUJ Alliance for Research and Enterprise, Energy and Energy-water Nexus Research Group, Campus for Research Excellence and Technological Enterprise, 138602, Singapore.

d. Science and Math Cluster, Singapore University of Technology and Design, 487372, Singapore

*Email: magdassi@mail.huji.ac.il

*Email: ge_qi@sutd.edu.sg

Table of Contents

1. Uniaxial tensile tests on PEGDA hydrogels

Tensile tests were conducted to measure the stress and stretch of hydrogel with varying PEGDA molecular weights (M_n) and water content on a MTS uniaxial tensile testing machine (Criterion Model 43, MN USA). PEGDA with different molecular weights were purchased from Sigma Aldrich in Singapore and used without further purification. The test was carried out by using samples with the dimension as 25 mm x 10 mm x 1 mm under 10 mm/min strain rate. Effects of PEGDA molecular weights and water content on stress-stretch behaviour of hydrogel are shown in Figures S1.

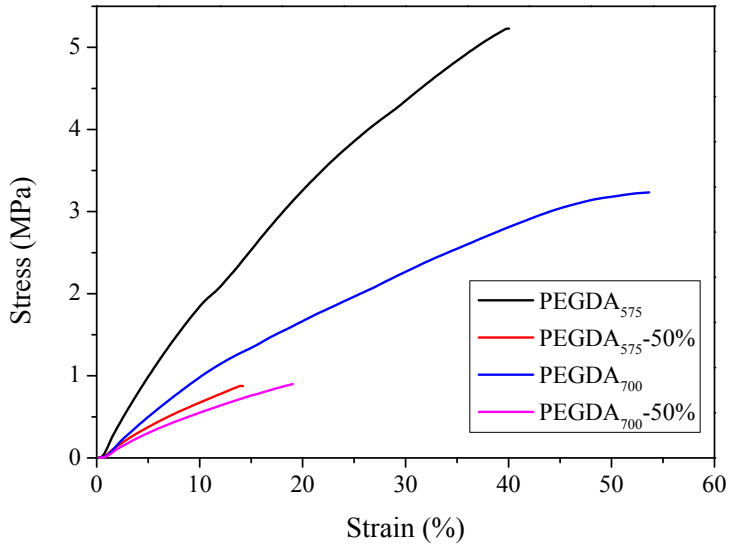

Figure S1. The tensile test results of PEGDA hydrogels. The break strain is 40%, 14%, 54% and 19% for PEGDA575, PEGA575-50% (50% water content), PEGDA700, PEGA700-50% (50% water content), respectively.

2. Preparation of TPO nanoparticles

TPO nanoparticles were prepared by drying of volatile microemulsions by spray dryer, which were reported elsewhere.[1] All the chemicals were purchased from Sigma Aldirch in Singapore and used directly. As shown in Figure S2, 2,4,6-tri-metylbenzoyl-diphenylphosphine oxide (TPO, 1.7 wt.%) was firstly dissolved in an "oil" (organic) phase, which were formed by mixing N-butyl acetate (nBuAc, 22.3 wt.%) with sodium dodecyl sulfate, (SDS, 7.5 wt.%), isopropyl alcohol (IPA, 7.5 wt.%) and polyvinylpyrrolidone (PVP, 7.5 wt.%). Here nBuAc works as the volatile solvent forming the microemulsion droplets; SDS is surfactant; IPA was selected as co-solvent and PVP is the crystallization inhibitor to prevent crystal growth of TPO during dispersion in water. Then the organic phase was mixed with water (40 w.t.%). The mixture was magnetically stirred at room temperature until clear systems was formed. The obtained microemulsions were spray dried by a Mini Spray Dryer B-290 equipped with inert loop dehumidifier B-296 (Buchi, Flawil, Switzerland). Theoretically, the resultant nanoparticle powders include 10 wt.% of TPO, 45 wt.% of SDS and 45 wt.% of PVP. These particles can be redispersed into water to get a clear solution by simple manual shaking for 2-5 min.

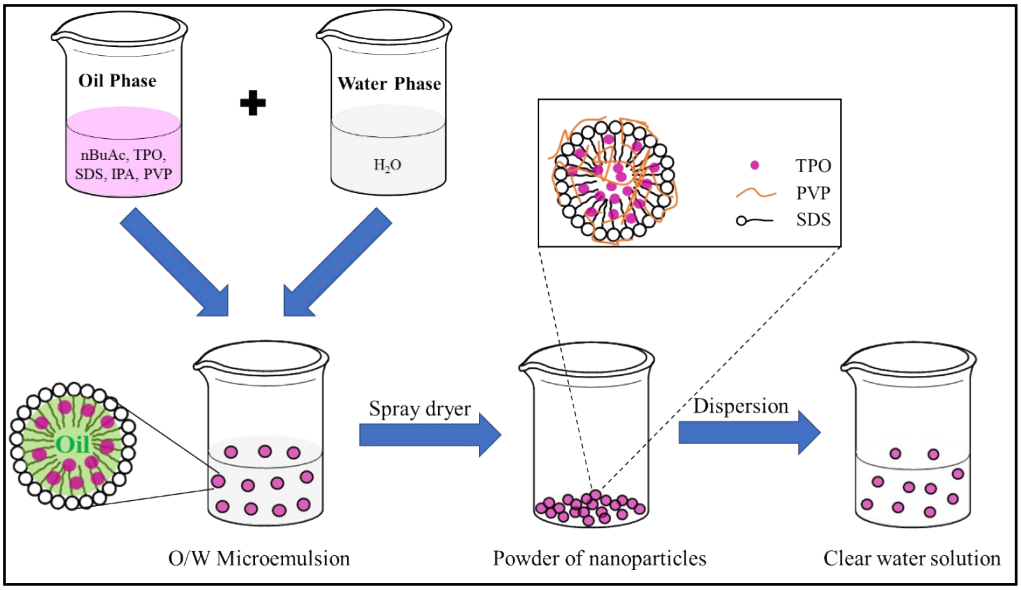

Figure S2. Schematic for preparing TPO nanoparticles by direct solvent evaporation using the spray drier.

3. Preparation of 3D Printing Solutions

Acrylamide, PEGDA and Sudan I were purchased from Sigma Aldrich. TPO-based nanoparticles was prepared according to the previously published proptocol.[1] Food coloring dyes were purchased from the local supermarket. TPO-based nanoparticles at 0.5 wt.% of acrylamide were first added into deionised water, and the mixture was stirred by magnetic stirrer for 10 minutes. Acrylamide was then added into the mixture and it was stirred for 5 minutes until completely dissolved. Photo absorber and PEGDA were added last. If Sudan I was used as the photo absorber, we dissolved Sudan I into PEGDA first, before adding the Sudan I-PEGDA mixture into the solution to achieve a desired weight ratio between PEGDA and acrylamide. Due to the low solubility of Sudan I in water, its weight content was kept at 0.015% of the overall solution. If food dye was used as the photo absorber, we added the pure PEGDA into the solution first, before adding the food dye (2 wt.% of the overall solution).

4. 3D Printing Apparatus

The hydrogel structures with mediate resolution (50-100 μm per pixel) were printed using a self-built 3D printing system with a CEL5500 LED light engine (405 nm, Digital Light Innovation, TX, USA) as the digital micro-display and a translation stage (LTS300) with 0.1 μm minimum achievable incremental movement and 2 μm backlash (Thorlabs, NJ, USA) as the elevator.[2] The printed layer thickness was set at 50 µm or 100 µm. The hydrogel structures with high resolution (2 μm) were printed using a commercial 3D printer (405 nm, nanoArch P130 3D printing system, BMF Material, China). The printed layer thickness was set 2 µm. The multimaterial 3D printing was realized by adding an automatic material exchange mechanism.[2-3] The printed gels were used in further studies as printed except cell viability tests.

5. Characterization of the activity of TPO nanoparticle as photoinitiator

To investigate the efficiency of these TPO nanoparticles, polymerization kinetics of the hydrogel solution consisting of 80 wt.% water, 20% Acrylamide-Polyethylene glycol diacrylate (PEGDA) mixture with the PEGDA (700)/acrylamide mixing ratio of 0.625 wt.%, and 0.5 wt. % TPO nanoparticles was measured by using Fourier-transform infrared (FT-IR) Spectrometer (Bruker, Germany) in conjunction with the single reflection attenuated total reflectance (ATR) accessory (64 scans with resolution at 4 cm^{-1}). To compare the efficiency, we also conducted polymerization kinetic tests of the same hydrogel solution with 0.5 wt.% of Irgacure 2959 (I2959, a commercial available water soluble photoinitiator) instead of TPO nanoparticles. The samples for polymerization kinetics were prepared by UV curing the aqueous solutions with a fix thickness of 140 µm under a near UV light (405 nm) for given time intervals. For each sample, IR spectra were recorded in the range 4000-400 cm^{-1}. The conversion of acrylamide was calculated from the decay/disappearance of the peak at 988 cm^{-1}, which is the out-of-plane bending mode of the =C-H unit (methylene group), normalized to the C=O stretching peak (carbonyl group) at 1655 cm^{-1} as an internal standard. Figure S3 shows the decay peaks of the methylene group after normalization for the hydrogel solutions with TPO nanoparticles and I2959 as the photoinitiator, respectively.

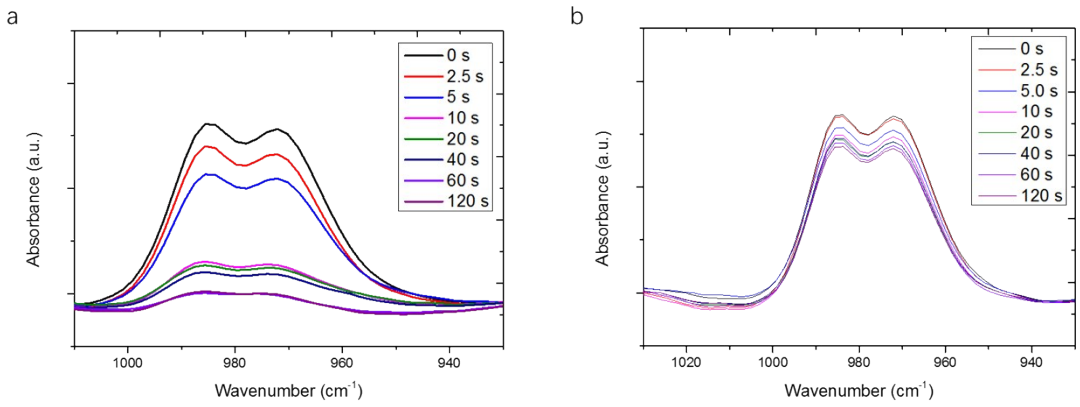

Figure S3. Polymerization kinetics. FT-IR of 3D printable acrylamide aqueous solutions with (a) TPO particles (930 - 1010 cm^{-1}) and (b) Irgacure 2959 (930 - 1030 cm^{-1}) obtained by exposing under UV (405 nm) for 0 s, 2,5 s, 5 s, 10 s, 20 s, 40 s, 60 s and 120 s.

6. Uniaxial tensile tests on AP hydrogels

Tensile tests were conducted to measure the stress and stretch of hydrogel with varying PEGDA concentrations, PEGDA molecular weights (Mn) and water content on a MTS uniaxial tensile testing machine (Criterion Model 43, MN USA). Figure S4a shows the geometry of the dog-bone sample used in the tests and the inset shows the black gauge points used to measure the axial stretch, λ, by using a digital-image-correlation (DIC) method. Effects of PEGDA concentrations, PEGDA molecular weights and water content on stress-stretch behaviour of hydrogel are shown in Figures S4b, c and d, respectively.

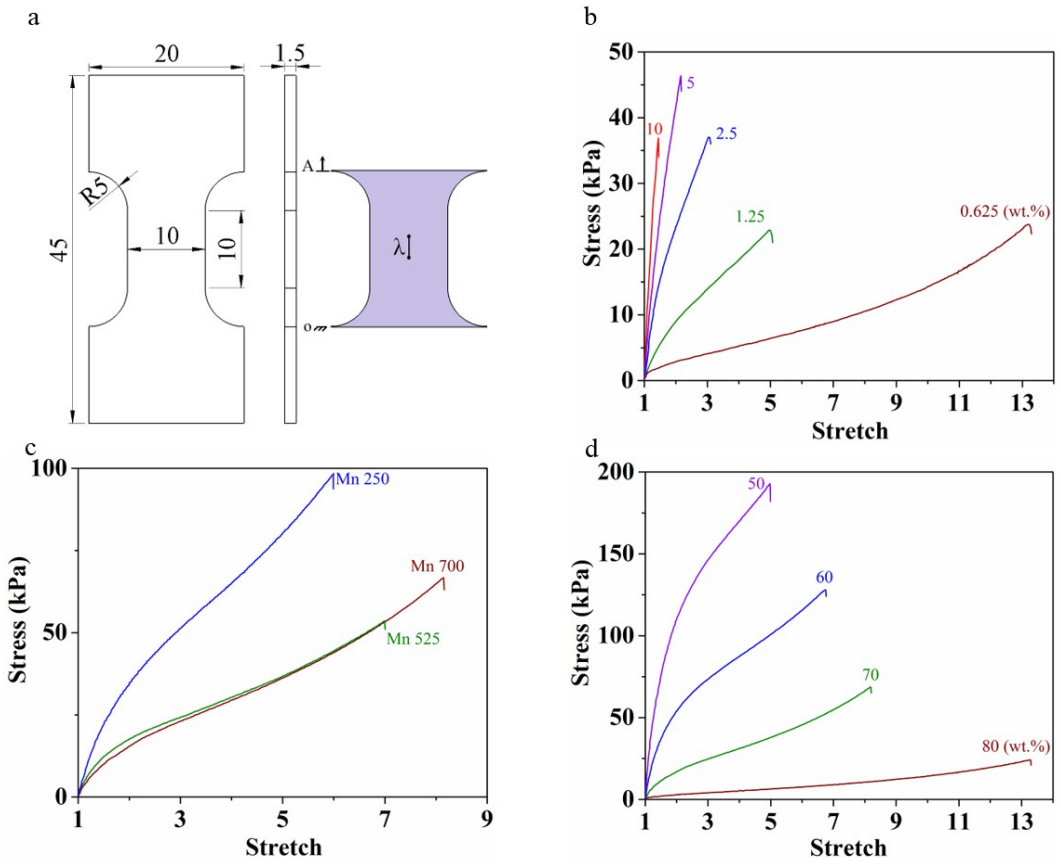

Figure S4. Uniaxial tensile tests on AP hydrogels. (a) Schematics of a hydrogel sample used for tensile test; The values are in mm; The inset shows the black gauge points used to measure the axial stretch, *λ*, by using a digital-image-correlation (DIC) method; The horizontal lines at "O" and "A" in the shoulder region indicate where the specimens were gripped at the shoulders of the dog-bone tension specimens. (b) Stress-stretch graph of hydrogel with varying wt. % PEGDA (700)/acrylamide at 80 wt.% water and 0.5 wt.% TPO-based nanoparticles; (c) Stress-stretch graph of hydrogel with varying PEGDA molecular weights at 70 wt.% water, 0.625 wt.% PEGDA/acrylamide and 0.5 wt.% TPO-based nanoparticles; (d) Stress-stretch graph of hydrogel with varying wt. % water at 0.625 wt.% PEGDA (700)/acrylamide and 0.5 wt.% TPO-based nanoparticles.

7. Curing time characterization

As illustrated in Figure S5a, a patterned near UV light with 405nm wavelength was irradiated onto the hydrogel pre-polymer solution which was sandwiched between two glass slides with a gap of 140 μm. After a time period, a hydrogel pattern (inset of Figure S5a) can be visually observed, and the time for UV irradiation is recorded as the curing time. Figure S5b shows the curing times for the AP hydrogel consisting of 80 wt.% water, 0.625 wt.% PEGDA(700)/acrylamide, 0.5 wt.% TPO nanoparticles with different PEGDA molecular weight and different concentrations of PEGDA. In Figure S5c, we also examined the effect of different dyes on the curing time. Sudan I at 0.015 wt.% and red and green food dyes at 1 wt.%, 2 wt.% and 4 wt.% were tested. Hydrogel solution was prepared with 60 wt.% water, 0.625 wt.% PEGDA (700)/acrylamide and 0.5 wt.% TPO-based nanoparticles.

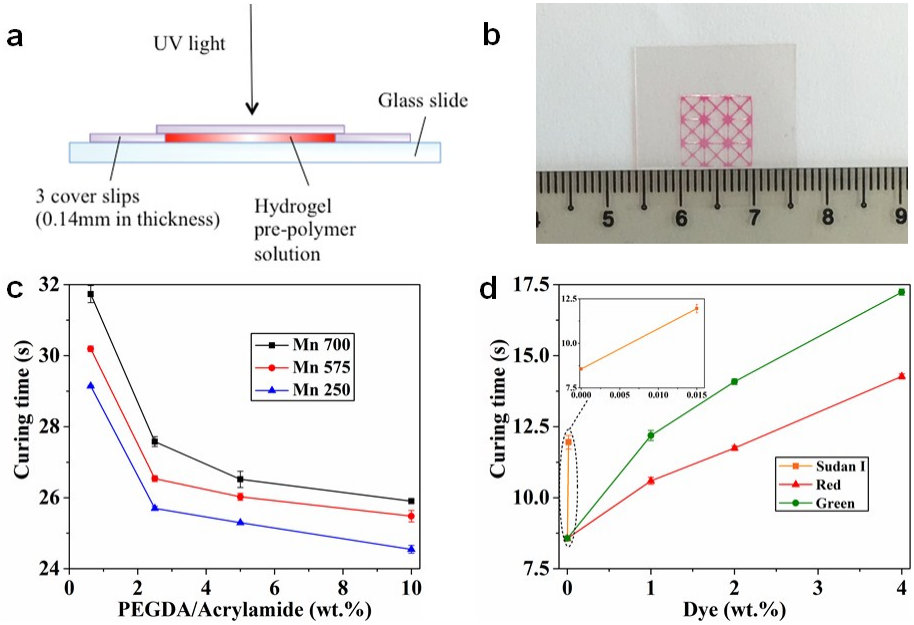

Figure S5. Curing time characterization. (a) Schematic of test to assess curing time. (b) curing time against different dyes at varying concentrations.

8. Mechanical tests on a hydrogel lattice structure

In order to facilitate the uniaxial tensile tests on the lattice structure, we designed and printed a pair of T-shape holders which can be easily mounted onto the testing machine's grippers. Figure S6a shows the details of the holder design. The holders were directly printed by a commercial multimaterial Polyjet 3D printer (Connex 500, Stratasys, MN, USA). The holders were made of a rigid material printing material (VeroWhite, Stratasys) and a flat thin (0.5 mm) elastomeric layer at the top/bottom to which the lattice is glued. The hydrogel based glue was prepared by mixing 50 wt.% water, 0.625 wt.% PEGDA (700)/Acrylamide, 0.5 wt.% TPO-based nanoparticles in terms of the weight of arylamide. After the lattice structure was printed, two droplets of the above-mentioned glue were pipetted onto the flat tango layer surface of the T-shape holder using a 1 ml disposable Pasteur pipette and quickly spread over the tango surface. The lattice structure was then placed onto the holder, and the whole structure was placed under the UV light (405 nm) for 45 seconds to glue the lattice to the holder. The same procedure was repeated on the other end of the lattice structure to obtain the final holder-lattice-holder structure (Figure 4b). After mounting the structure on the grippers of the MTS uniaxial tensile machine, the test was conducted at the rate of 1.5 mm/s (Movie S3).

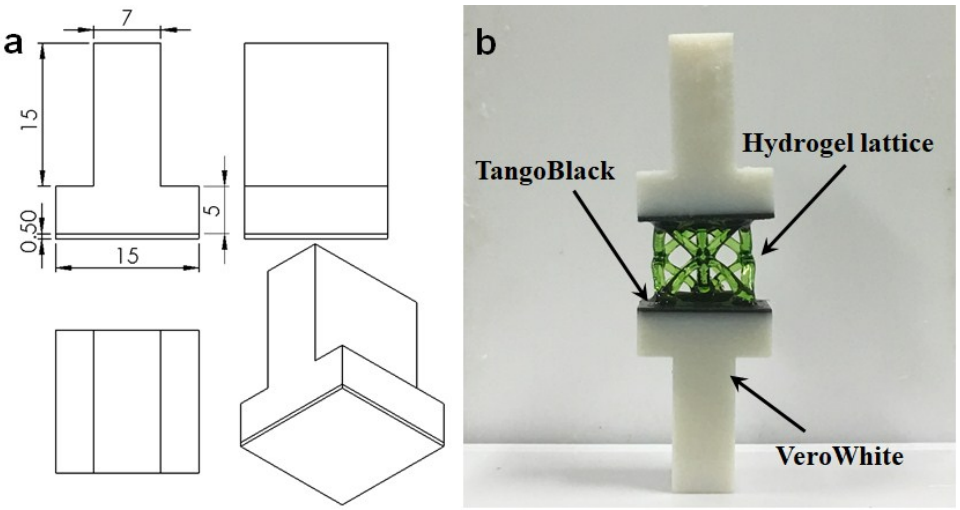

Figure S6. T-shape holders for lattice structure tests. (a) Details of the holder design. (b) The picture shows that the printed lattice structure is attached to the T-shape holders for the mechanical test.

9. Finite element simulation on hydrogel lattice structure

To investigate the local deformation on the deformed hydrogel lattice structures under tension, the finite element simulation was performed using a commercial finite element software, (Simulia, Providence, RI, USA). The hydrogel is modelled simply by the hyperelastic Mooney-Rivlin model, and the geometry is meshed using four-node three-dimensional linear tetrahedron elements with hybrid formulation (C3D4H) within ABAQUS software. The generalized Mooney–Rivlin constitutive model was employed to represent the hyperelastic behavior of hydrogel. The form of the Mooney–Rivlin strain energy potential is $U = C_{10}\left(\bar{I}_1 - 3\right) + C_{01}\left(\bar{I}_2 - 3\right) + D_1^{-1}\left(J-1\right)^2$, where U is the strain energy density, C_{10}, C_{01}, and D_1 are material parameters. $\bar{I}_1$, $\bar{I}_2$ and J are the three principal invariants of the left Cauchy-Green deformation tensor $\mathbf{B}$, and are defined as $\bar{I}_1 = J^{-2/3}B_{kk}$, $\bar{I}_2 = \left(\bar{I}_1^2 - J^{-3/4}B_{ik}B_{ki}\right)/2$, and $J = \sqrt{\det(\mathbf{B})}$, where $\mathbf{B} = \mathbf{F}\mathbf{F}^T$ and $\mathbf{B}$ is the deformation gradient tensor. Then, the stress-strain relation can be represented as $\sigma_{ij} = 2J^{-5/3}C_{10}\left(B_{ij} - B_{kk}\delta_{ij}/3\right) + 2J^{7/3}C_{01}[B_{kk}B_{ij} - B_{kk}^2\delta_{ij}/3 - B_{ik}B_{kj} + B_{kn}B_{nk}\delta_{ij}/3] + 2D_1^{-1}\left(J-1\right)\delta_{ij}$. The material parameters, C_{10}, C_{01}, and D_1 were defined by fitting this model with uniaxial experimental data for hydrogel as can be seen in Figure S7. The obtained values for the material parameters are 1.02×10^{-2} MPa, 3.8×10^{-2} MPa, and 2.07 MPa^{-1} for C_{10}, C_{01}, and D_1, respectively.

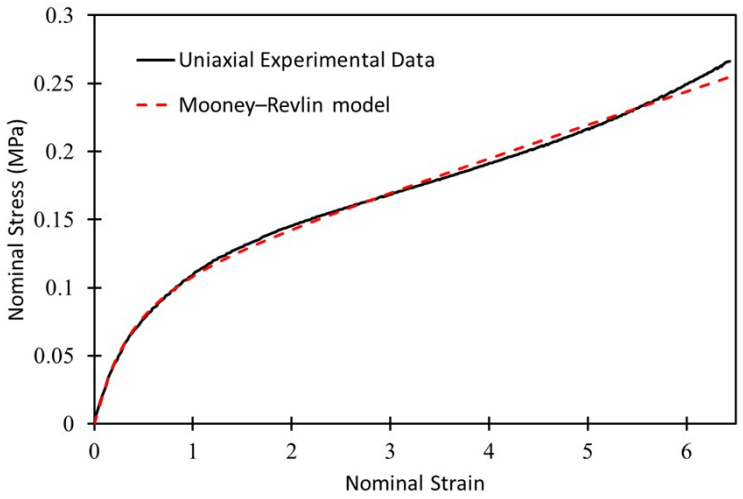

Figure S7. The fitted Mooney–Revlin model for hydrogel material with uniaxial experimental data.

10. Cell Viability Tests

Both HepG2 liver cancer cell and NIH 3T3 cells were cultured in Dulbecco's modified eagle medium (DMEM) (high glucose) (Sigma Aldrich, Singapore) supplemented with 10% fetal bovine serum (FBS) (Gibco-Invitrogen, Carlsbad, CA, USA). NIT-3T3 cells from passage 5-8 were used in the experiment, and they were grown in a humidified 5% CO_2 incubator at 37 °C. Hydrogels slabs were prepared with dimensions of ~ 4 mm in length, ~ 4 mm in width, and 0.3 mm in thickness. The prepared hydrogel slabs for cell viability tests are made of 80 wt.% water, 20 wt.% acrylamide-PEGDA mixture with PEGDA(700)/mixing ration at 33.3 wt.%. Hydrogels were sterilized by exposing to UV light in the biological safety cabinet for 20 minutes before exposed to the cell culture medium. The hydrogels were exposed to 300 μL cell culture medium in individual wells overnight. The medium was replaced before cells were seeded into each well containing a slab of hydrogel. Cells were trypsinized with 0.25% trypsin–ethylenediaminetetraacetic acid (EDTA) (Gibco-Invitrogen, Carlsbad, CA, USA) and mixed with culture medium before seeding. HepG2 cells were seeded at a concentration of 2×10^6 mL^{-1} cells per well and NIH-3T3 cells were seeded a concentration of 1.35×10^5 mL^{-1} cells per well. Cells were cultured for 7 days and assayed on day 1, 3, 5 and 7 post seeding. A live/dead viability assay (Invitrogen, Carlsbad, CA, USA) consisting calcein-AM/ethidium homodimer was used to analyze the cells within the well, according to the manufacturer's protocol. Images were visualized by fluorescence microscope (CKX53, Olympus, Tokyo, Japan). Pictures were taken from 4 corners of the hydrogel slab within the well, the average value of 4 counts were reported for each reading. Florescence images were split into red, green and blue channel and converted into 8-bit greyscale using Fiji software. Cells were counted by applying the "find maxima" function in Fiji software. The output value is known as counts and is recorded for the red channel and green channel. The counts in the green channel represent live cells and the counts in the red channel represent dead cells. The viability per sample was determined by the total count of live cells divided by the total cells present (live and dead cells).

Sodium dodecyl sulfate (SDS) in TPO-nanoparticle is toxic, but the cell viability test results proved the excellent biocompatibility of the hydrogels. The reason is that the concentration of SDS in our hydrogel system is very low. As the prepared hydrogel slabs for cell viability tests are made of 80 wt.% water, 20 wt.% acrylamide-PEGDA mixture with PEGDA(700)/mixing ration at 33.3 wt.%, only around 0.03 wt.% of SDS is included in the prepared hydrogel slabs, far below its corresponding critical micelle concentration (CMC), which shows toxicity.[4]

To confirm our conclusion, we carried out FT-IR experiments (Fig. 1). From the spectrum of SDS, we can clearly see the strong absorption peak at 1220 cm-1, which is attributed to skeletal vibration involving the bridge S–O stretch.[5] While there is no visible absorption peak at 1220 cm-1 from the infrared spectra of the printed hydrogel and the treated hydrogel for cell culture, which prove that there are minimal/no SDS in the printed hydrogel and the treated hydrogel for cell culture.

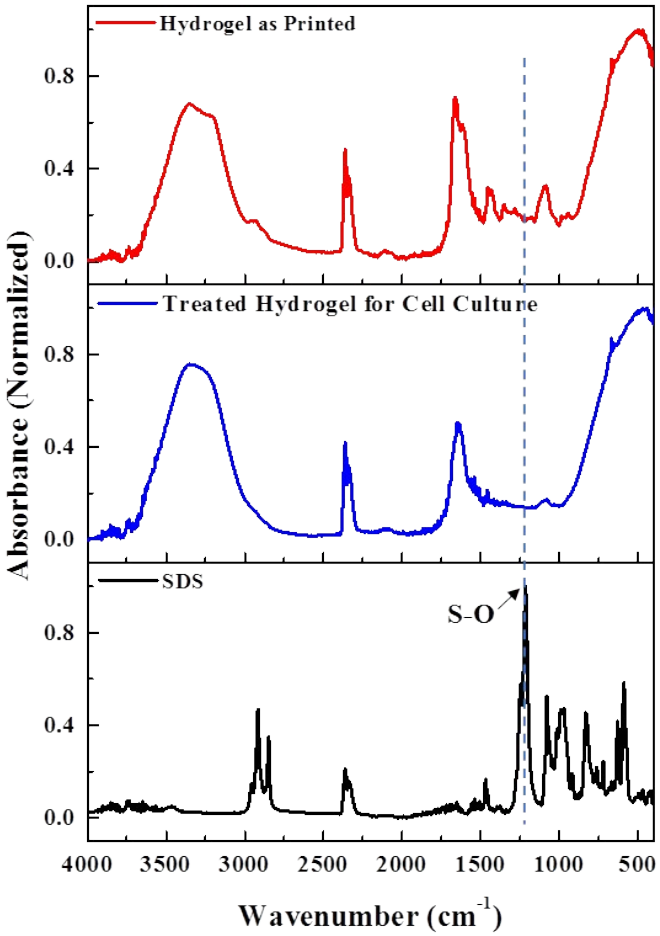

Figure S8. FT-IR spectra of the hydrogel as printed (up), the treated hydrogel for cell culture (middle) and sodium dodecyl sulfate (SDS) powder (bottom). Fourier Transform Infrared Spectroscopy (FT-IR) tests were conducted on a VERTEX 70 FT-IR spectrometer (Bruker, Germany) using Attenuated Total Reflection (ATR) mode with a Magna-IR Nicolet 550 collecting 32 scans from 400 to 4000 cm^{-1}.

11. Light transmittance tests

The transmittance tests were conducted using a spectrophotometer (LAMBDA™ 750 UV/Vis/NIR PerkinElmer, MA, USA). The spectra from 250 nm to 800 nm were scanned at a rate of 266.75 nm/min. The thickness of the hydrogel thin films for the tests was 1 mm.

12. Schematic illustration of the strong interface

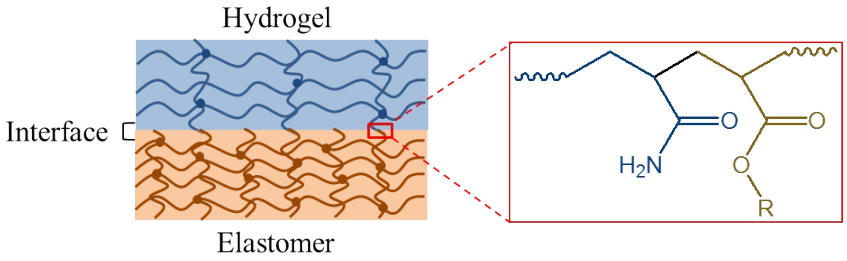

Figure S9. The proposed bonding mechanism between hydrogel and elastomer.

Table S1. Summary of printing techniques, materials, printed resolution, and tensile properties for 3D printable hydrogels.

Technique	Material	Specified resolution [μm]	Young's Modulus [kPa]	Break strain [%]	Reference
Extrusion Based +Post UV cured	Agar/PAAm/ Alginate	455 - 1200	70 - 870	224 - 1017	[6]
Extrusion Based +Post UV cured	PEGDA	830	5.3 - 74.6	50 - 150	[7]
Extrusion Based +Post UV cured	PAAm/Alginate	337	48 - 83	90 - 300	[8]
Extrusion Based +Post UV cured	PEG/Alginate/Nanoclay	~ 500	–	~300	[9]
Extrusion Based (Bio-plotting)	Alginate/Gelatin	200	20 - 90	~ 15	[10]
Extrusion Based +Post UV cured	PEGX/Natural polymers	200	48.3	~ 400	[11]
Dynamic optical projection stereolithography (DOPsL)	PEGDA PEGDA/Nanoparticles	~1	–	–	[12-15]
Extrusion Based (3D bioprinter)	Gelatin/Alginate	800	1.44	~ 55	[16]
Direct Laser Bioprinting	GelMa	400	–	–	[17]
SLA 3D printer	AAm/Ethoxylated trimethylolpropane	39	–	–	[1]
Extrusion Based (3D bioprinter)	Agarose/SWCNT	~ 500	20 - 700	>15%	[18]
Digital Mirror Device (DMD) based modulating projection printing	PEGDA	1.36	25 - 125	–	[19]
Extrusion Based (3D bioprinter)	PEGDA/Alginate GelMA/Alginate Et al.	~100 - 200	–	–	[20]
Extrusion Based (3D bioprinter)	Alginate/Gelatin	400	–	–	[21]
Extrusion Based (3D bioprinter)	Alginate/Chondrocytes	–	14 - 114	<20%	[22]

Digital Light Processing	PEGDA/Enzymes/Antibody	50	–	–	[23]
Extrusion Based (3D bioprinter)	Alginate/Gelatin etal.	~100	–	–	[24,25]
Extrusion Based (3D bioprinter)	Gelatin/Fibrinogen/HA/PCL Gelatin/Fibrinogen/HA/Cells	2 50	– –	– –	[26]
Extrusion Based +Post UV cured	PAAm/α-keto/TEMED	500	–	~150	[27]
Extrusion Based +Post UV cured	GelMA	30 - 200	–	–	[28]
Extrusion Based +Post UV cured	DMAAm/ NIPAAm/NFC	150 - 1500	1011 - 1267	67 - 140	[29]
2PP	GelMA, PEGDA, PEGDA/HEMA, HA, BSA, etal.	0.3 - 5	–	–	[30,31]
Digital Light Processing	NIPAM	30	–	–	[32]

Note: PEG: Poly(ethylene glycol); PEGDA: Poly(ethylene glycol) diacrylate; PAAm: Poly(Acrylamide); SWCNT: single-walled carbon nanotubes; HA: hyaluronic acid; GelMA: Gelatin Methacrylate; DMAAm: N,N-dimethylacrylamide; NIPAAm: N-isopropylacrylamide; NFC: nanofibrillated cellulose; α-ketoglutaric acid: α-keto; N,N,N′,N′-tetramethylethylenediamine: TEMED; PCL: Polycaprolactone; HEMA: 2-Hydroxiethyl methacrylate; BSA: Bovine serum albumin.

References

1 A. A. Pawar, G. Saada, I. Cooperstein, L. Larush, J. A. Jackman, S. R. Tabaei, N.-J. Cho, S. Magdassi, *Sci. Adv. 2016,* **2,** e1501381.

2 Q. Ge, A. H. Sakhaei, H. Lee, C. K. Dunn, N. X. Fang, M. L. Dunn, *Sci. Rep.*, 2016, **6**, 31110.

3 Q. Wang, J. A. Jackson, Q. Ge, J. B. Hopkins, C. M. Spadaccini, N. X. Fang, *Phys. Rev. Lett*., 2016, **117**, 175901.

4 A. S. Inacio, K. A. Mesquita, M. Baptista, J. Ramalho-Santos, W. L. C. Vaz, O. V. Vieira, *PLoS One,* 2011, **6(5),** e19850.

5 M. K. Singh, A. Agarwal, R. Gopal, R. K. Swarnkar, R. K. Kotnala, *J. Mater. Chem.,* 2011, **21,** 11074.

6 J. Wei, J. Wang, S. Su, S. Wang, J. Qiu, Z. Zhang, G. Christopher, F. Ning, W. Cong, *RSC Adv.,* 2015, **5**, 81324.

7 L. Hockaday, K. Kang, N. Colangelo, P. Cheung, B. Duan, E. Malone, J. Wu, L. Girardi, L. Bonassar, H. Lipson, *Biofabrication,* 2012, **4**, 035005.

8 S. E. Bakarich, S. Beirne, G. G. Wallace, G. M. Spinks, *J. Mater. Chem*., B 2013, **1**, 4939.

9 S. Hong, D. Sycks, H. F. Chan, S. Lin, G. P. Lopez, F. Guilak, K. W. Leong, X. Zhao, *Adv. Mater*., 2015, **27**, 4035.

10 F. You, X. Wu, X. Chen, *Int. J. Polym. Mater*., 2017, **66**, 299.

11 A. L. Rutz, K. E. Hyland, A. E. Jakus, W. R. Burghardt, R. N. Shah, *Adv. Mater*., 2015, **27**, 1607.

12 J. Warner, P. Soman, W. Zhu, M. Tom, S. Chen, *ACS Biomater. Sci. Eng*., 2016, **2**, 1763.

13 A. P. Zhang, X. Qu, P. Soman, K. C. Hribar, J. W. Lee, S. Chen, S. He, *Adv. Mater*., 2012, **24**, 4266.

14 W. Zhu, J. Li, Y. J. Leong, I. Rozen, X. Qu, R. Dong, Z. Wu, W. Gao, P. H. Chung, J. Wang, *Adv. Mater*., 2015, **27**, 4411.

15 M. Gou, X. Qu, W. Zhu, M. Xiang, J. Yang, K. Zhang, Y. Wei, S. Chen, *Nat. Comm*., 2014, **5**, 3774.

16 B. Duan, L. A. Hockaday, K. H. Kang, J. T. Butcher, *J. Biomed. Mater. Res., A* 2013, **101**, 1255.

17 Z. Wang, X. Jin, R. Dai, J. F. Holzman, K. Kim, *RSC Adv.,* 2016, **6**, 21099.

18 A. Nadernezhad, N. Khani, G. A. Skvortsov, B. Toprakhisar, E. Bakirci, Y. Menceloglu, S. Unal, B. Koc, *Sci. Rep.,* 2016, **6**, 33178.

19 W. Yang, H. Yu, W. Liang, Y. Wang, L. Liu, *Micromachines,* 2015, **6**, 1903.

20 W. Liu, Y. S. Zhang, M. A. Heinrich, F. De Ferrari, H. L. Jang, S. M. Bakht, M. M. Alvarez, J. Yang, Y. C. Li, G. Trujillo-de Santiago, *Adv. Mater.,* 2017, **29**.

21 Y. He, F. Yang, H. Zhao, Q. Gao, B. Xia, J. Fu, *Sci. Rep.,* 2016, **6**, 29977.

22 M. S. Mannoor, Z. Jiang, T. James, Y. L. Kong, K. A. Malatesta, W. O. Soboyejo, N. Verma, D. H. Gracias, M. C. McAlpine, *Nano Lett.,* 2013, **13**, 2634.

23 C. l. A. Mandon, L. J. Blum, C. A. Marquette, *Anal. Chem.,* 2016, **88**, 10767.

24 K. Arai, Y. Tsukamoto, H. Yoshida, H. Sanae, T. A. Mir, S. Sakai, T. Yoshida, M. Okabe, T. Nikaido, M. Taya, *Int. J. Bioprint.,* 2016, **2**, 153.

25 K. Arai, S. Iwanaga, H. Toda, C. Genci, Y. Nishiyama, M. Nakamura, *Biofabrication,* 2011, **3**, 034113.

26 H.-W. Kang, S. J. Lee, I. K. Ko, C. Kengla, J. J. Yoo, A. Atala, *Nat. Biotechnol.,* 2016, **34**, 312.

27 K. Tian, J. Bae, S. E. Bakarich, C. Yang, R. D. Gately, G. M. Spinks, Z. Suo, J. J. Vlassak, *Adv. Mater.,* 2017, **29**.

28 D. B. Kolesky, R. L. Truby, A. Gladman, T. A. Busbee, K. A. Homan, J. A. Lewis, *Adv. Mater.,* 2014, **26**, 3124.

29 A. S. Gladman, E. A. Matsumoto, R. G. Nuzzo, L. Mahadevan, J. A. Lewis, *Nat. Mater.,* 2016, **15**, 413.

30 A. Ovsianikov, A. Deiwick, S. Van Vlierberghe, P. Dubruel, L. Möller, G. Dräger, B. Chichkov, *Biomacromolecules,* 2011, **12**, 851.

31 A. I. Ciuciu, P. J. Cywiński, *RSC Adv.,* 2014, **4**, 45504.

32 D. Han, Z. Lu, S. A. Chester, H. Lee, *Sci. Rep.,* 2018, **8**, 1963.

List of Movies

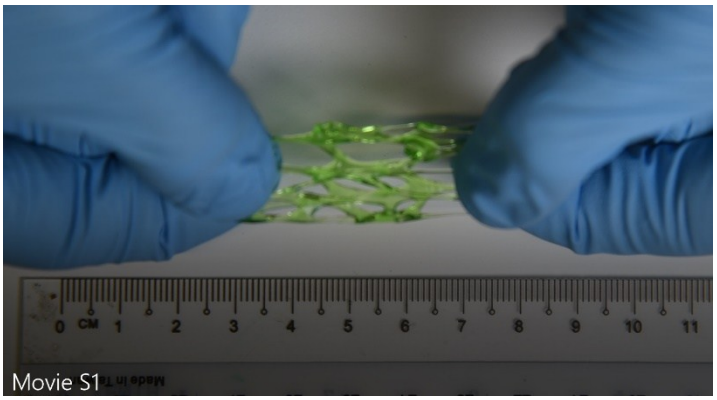

Movie S1. A printed Bucky ball under a large deformation.

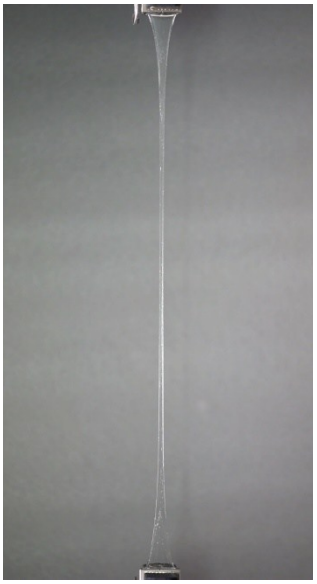

Movie S2. High stretchability of 3D printed hydrogel strip sample.

Movie S3. Stretching a 3D printed hydrogel lattice structure.

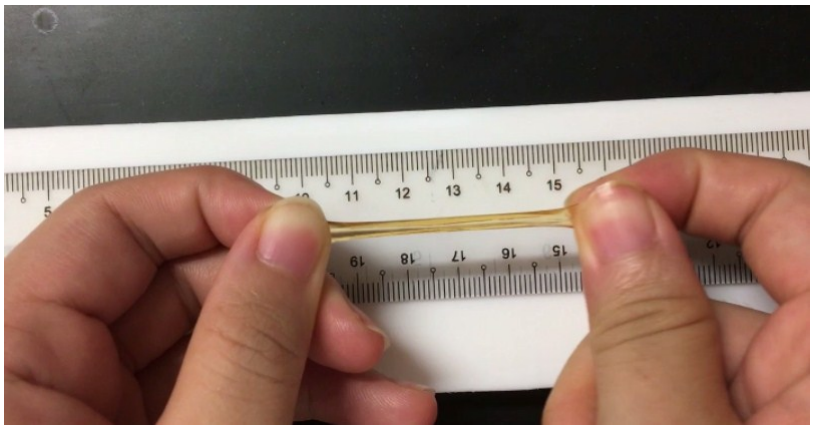

Movie S4. Stretching a 3D printed blood vessel.

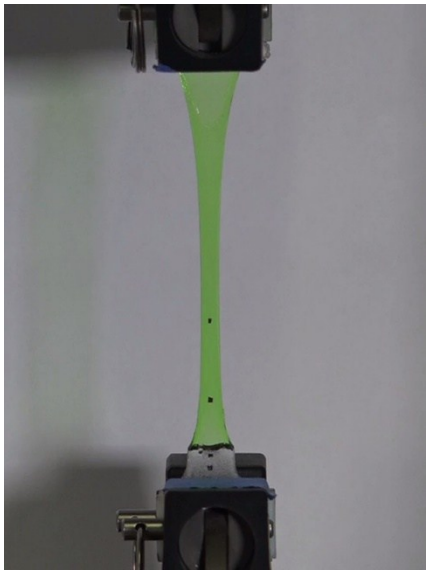

Movie S5. Stretching a 3D hydogel-elastomer hybrid.

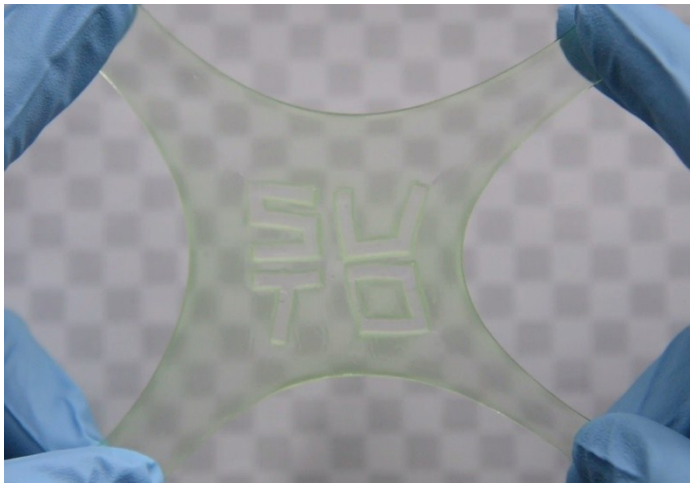

Movie S6. Stretching a hydrogel sheet with the elastomeric “SUTD” letters embedded.

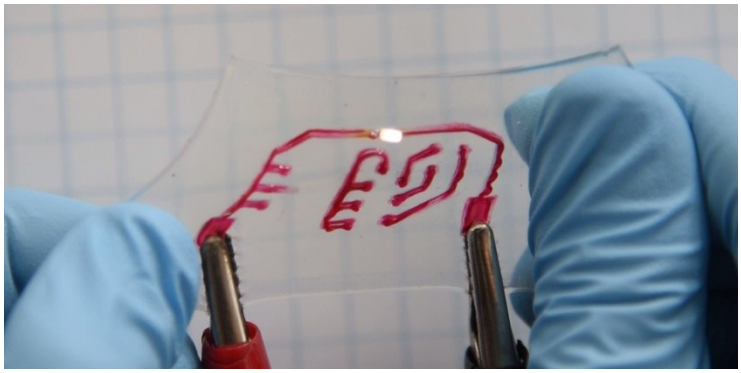

Movie S7. A stretchable electronic board with a printed conductive hydrogel circuit.